Article

pubs.acs.org/Biomac

Immobilization of Coacervate Microcapsules in Multilayer Sodium Alginate Beads for Efficient Oral Anticancer Drug Delivery

Chao Feng,[†] Ruixi Song,[†] Guohui Sun,[†] Ming Kong,[†] Zixian Bao,[†] Yang Li,[†] Xiaojie Cheng,[†] Dongsu Cha,[‡] Hyunjin Park,*[,‡] and Xiguang Chen*[,†]

[†]College of Marine Life Science, Ocean University of China, Yushan Road, Qingdao 266003, Shandong Province, People's Republic of China

[‡]Graduate School Biotechnology, Korea University, 1,5-Ka, Anam-Dong, Sungbuk-Ku, Seoul 136-701, South Korea

Supporting Information

ABSTRACT: We have designed and evaluated coacervate microcapsules-immobilized multilayer sodium alginate beads (CMs-M-ALG-Beads) for oral drug delivery. The CMs-M-ALG-Beads were prepared by immobilization of doxorubicin hydrochloride (DOX) loaded chitosan/carboxymethyl coacervate microcapsules (DOX:CS/CMCS-CMs) in the core and layers of the multilayer sodium alginate beads. The obtained CMs-M-ALG-beads exhibited layer-by-layer structure and rough surface with many nanoscale particles. The swelling characteristic and drug release results indicated that 4-layer CMs-M-ALG-Beads possessed favorable gastric acid tolerance (the swelling rate <5%, the cumulative drug release rate <3.8%). In small intestine, the intact DOX:CS/CMCS-CMs were able to rapidly release from CMs-M-ALG-Beads with the dissolution of ALG matrix. Ex vivo intestinal mucoadhesive and permeation showed that CMs-M-ALG-Beads exhibited continued growth for P_{app} values of DOX, which was 1.07−1.15 folds and 1.28−1.38 folds higher than DOX:CS:CMCS-CMs in rat jejunum and ileum, respectively, demonstrating that CMs-M-ALG-Beads were able to enhance the absorption of DOX by controlled releasing DOX:CS/CMCS-CMs and prolonging the contact time between the DOX:CS/CMCS-CMs and small intestinal mucosa.

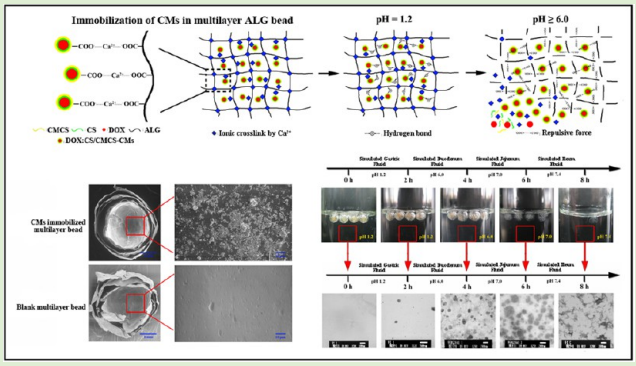

INTRODUCTION

Intravenous administration of anticancer drug remains to be the most prevalent approach for the treatment of tumors.[1−3] Nonetheless, the intravenous administration often results in limited therapeutic effects due to the impulse concentration of a drug in systemic circulation and poor patient compliance.[4] Oral administration of anticancer drug is a viable alternative to intravenous injections, since it can maintain an optimum blood drug concentration to improve efficacy as well as decrease corresponding side effects;[5,6] in addition, patients are more receptive to it.[1,7] Nevertheless, delivering anticancer drug orally often leads to a low bioavailability owing to first-pass effect and barriers to physical absorption in the epithelium.[4,8]

In our recent work, pH-responsive coacervate microcapsules (CS/CMCS-CMs) composed of chitosan (CS) and carboxymethyl chitosan (CMCS) were developed for oral deliver anticancer drug.[9] CS, a mucoadhesive polycation, can enhance the intestinal paracellular permeability by transiently opening the tight junctions (TJs). CMCS disrupts epithelial TJs by nonspecific chelation of divalent Ca^{2+} ions thus expands the range of the absorption enhancement from limited duodenal segment to the entire small intestine.[10] The stability of CS/CMCS-CMs was closely related to the electrostatic interaction between protonated amine groups on CS and deprotonated carboxyl groups on CMCS. The pK_a of amine groups on CS and carboxyl groups on CMCS is approximately 6.5 and 2.0−4.0, respectively. Hence, the prepared CS/CMCS-CMs remained intact in pH range of 2.0−7.0; however, outside of this range, they became unstable, resulting in premature drug release in gastric acid environment (pH 1.2−2.5) and precipitation after storage in deionized (DI) water (pH 7.0) in few days.[9] The undesirable release of drug could not be absorbed in the small intestine without assistance of CS/CMCS-CMs and might have potential toxicity for gastrointestinal tissue. Increasing the stability of DOX:CS/CMCS-CMs in a broader pH range and maintaining their dispersing state are thus essential to further increase the efficacy of CS/CMCS-CMs for oral delivery of anticancer drug.

To overcome these problems, a pH-sensitive oral drug delivery system of DOX:CS/CMCS-CM-immobilized multilayer sodium alginate beads (CMs-M-ALG-Beads) was prepared by dropping aqueous DOX:CS/CMCS-CMs blended with alginate (ALG) into Ca^{2+} solution. The basic concept is that the ALG matrix protects encapsulated DOX:CS/CMCS-CMs from gastric juices,[11,12] and rapidly releases the intact DOX:CS/CMCS-CMs in the neutral (or slightly basic) environment of the small

Received: December 21, 2013
Revised: February 2, 2014

   dx.doi.org/10.1021/bm401890x | Biomacromolecules XXXX, XXX, XXX−XXX

Scheme 1. Preparation of DOX:CS/CMCS-CM-Immobilized Multilayer ALG Beads

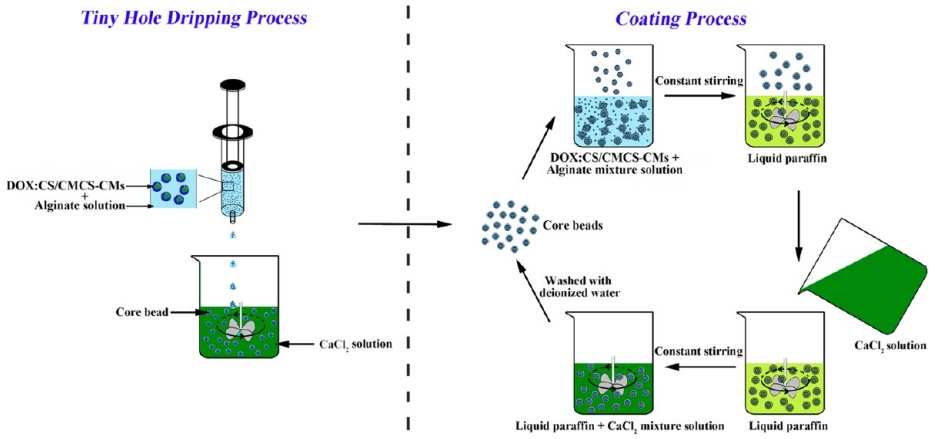

intestine. The layer-by-layer (LBL) technology has been utilized to form the multilayer ALG beads. Immobilization of DOX:CS/CMCS-CMs in the core of multilayer ALG bead can overcome the problem of high initial burst release commonly encountered in encapsulated beads.[13,14] Meanwhile, drug release rate are expected to be controlled by controlling the number of layers, thereby potentially enhancing drug delivery efficacy.[15,16]

In this study, the morphology and swelling property of the CMs-M-ALG-Beads were characterized by scanning electron microscopy (SEM) and a gravimetric method, respectively. The drug loading level was optimized by response surface method using doxorubicin hydrochloride (DOX) as a model drug. The stability, release profiles of DOX were evaluated in simulated gastric and intestinal fluid. Finally, the mucoadhesive and intestinal permeation properties of this drug delivery system were also studied in vitro.

MATERIALS AND METHODS

Reagents and Materials. CS (molecular weight, MW: 10 kDa, degree of deacetylation, DD: 89%) was obtained from Biotech Co. (Mokpo, Korea). CMCS (MW: 12 kDa, DD: 81%, degree of substitution, DS: 92%) was synthesized and characterized by the method described by Chen.[17] Sodium alginate, calcium chloride, and liquid paraffin were purchased from Sinopharm Chemical Reagent Co., Ltd. (Shanghai, China). Span 80 and Tween 80 were purchased from Solarbio (Beijing, China). DOX was supplied by Zhejiang Hai Zheng Co. Ltd. (China). All other reagents and solvents were of analytical grade.

Preparation of DOX-Loaded CS/CMCS-CMs. DOX-loaded CS/CMCS-CMs (DOX:CS/CMCS-CMs) were prepared according to a modified process originally based on our previous work.[9] Briefly, DOX aqueous solution (1 mg/mL, 1 mL) was premixed with CS (1 mg/mL, 4 mL) under magnetic stirring for 30 min. Subsequently, CMCS solution (1 mg/mL, 3 mL, pH 6.6) and TPP (0.25 mg/mL, 2 mL) were blended with the mixture under constant stirring for 1 h, and DOX:CS/CMCS-CMs formed.

Preparation of DOX:CS/CMCS-CM-Immobilized Multilayer Sodium Alginate Beads. DOX:CS/CMCS-CM-immobilized multilayer sodium alginate beads (CMs-M-ALG-Beads) were prepared by the LBL method, which was divided into two processes (Scheme 1). In the tiny hole dropping process, 1 mL of fresh DOX:CS/CMCS-CMs (0.1%, 0.3% or 0.5% w/v) were premixed with various concentrations of sodium alginate solution (ALG, 1%, 3% or 5%, w/v) under magnetic stirring for 2 h. Then, the mixture solution was dropped into $CaCl_2$ solution (1%, 3% or 5%, w/v) by a glass syringe without a needle at a dropping rate of 1.0 mL/min under stirring (100 rpm) for 30 min to form the core of bead. The prepared core beads were removed from the solution and washed the residual $CaCl_2$ with distilled water. During the coating process, the cores were immersed in a corresponding ALG and DOX:CS/CMCS-CMs mixture solution for 5 min. Then the mixture solution with the prepared core beads was poured into liquid paraffin (oil phase) contained Span 80 (0.6 mL) and Tween 80 (0.2 mL) in advance while stirring (300 rpm). The $CaCl_2$ solution was then added to the mixture 10 min later and stirred for another 30 min to form 1-layer CMs-M-ALG-Beads. Then the 1-layer beads were taken out from the mixture and rinsed with distilled water until the liquid paraffin was removed completely. The coating process was repeated until the multilayer beads with the required number of layers were prepared, then freeze-dried. The number of layers was equal to the number of repeats of the coating process.

Characterization. CMs-M-ALG-Beads were respectively incubated in buffer solution at different pH (tris-HCl at pH 1.2, PBS at pH 6.0, PBS at pH 7.0) and gently shaken in a thermostatted shaker bath for 1 h (37 °C, 50 rpm), then dried and analyzed by Fourier transform infrared spectroscopy (FTIR, Nicolet, 5DX/550II, USA) with a disk of KBr.

The size of beads was determined with calipers. A diameter of at least 100 beads was determined to calculate the average diameter. The mean of diameter (D) was calculated using eq 1

$$D = \sum nd/nn \geq 100 \quad (1)$$

where d is the diameter of each beads, n is the total number of beads measured, and D is the mean diameter.

The morphologies of multilayer ALG beads with and without DOX:CS/CMCS-CMs were observed via scanning electron microscope (SEM, JSM-6010LA, JEOL Ltd., Japan), fluorescence microscopy (Nikon Eclipse Ti−S, Nikon Ltd., Japan), and confocal laser scanning microscopy (CLSM, LSM510, Zeiss Ltd., Germany), respectively.

Optimization of CMs-M-ALG-Beads. Optimization of CMs-M-ALG-Beads was completed using response surface methodology (RSM), which is a statistical and mathematical method used to fit the experimental data to the model for optimization processes.[18] A response surface method, Box−Behnken experimental design (BBD), was used to statistically optimize the formulation parameters and evaluate the main effects, interaction effects, and quadratic effects of the formulation ingredients on the encapsulation efficiency (EE) of multilayer bead.[19]

A three-factor, three-level design was used to explore the quadratic response surfaces and for constructing second-order polynomial models using Design Expert (Version 7.0.0, Stat-Ease Inc., Minneapolis, MN). The independent variables, including the concentration of sodium alginate (A), calcium chloride (B), and DOX:CS/CMCS-CMs (C) were defined in three levels (low, medium and high). Seventeen experiments, including 12 factorial points with five replicates at the center point for estimation of pure error sum of squares, were employed. The ranges of levels of the independent variables and the design matrix are shown in Tables 2 and 3, respectively. The mathematical relationship of the responses (Y, EE) and the independent variables (X_i) were modeled by a second-order polynomial function as follows:

dx.doi.org/10.1021/bm401890x | Biomacromolecules XXXX, XXX, XXX−XXX

$$Y = \alpha_0 + \alpha_1 X_1 + \alpha_2 X_2 + \alpha_3 X_3 + \alpha_{11} X_1^2 + \alpha_{22} X_2^2 + \alpha_{33} X_3^2 + \alpha_{12} X_1 X_2 + \alpha_{13} X_1 X_3 + \alpha_{23} X_2 X_3$$

where Y is the predicted response; α_0 is an intercept; α_1, α_2, and α_3 are linear coefficients, α_{11}, α_{22}, and α_{33} are squared coefficients; α_{12}, α_{13}, and α_{23} are the interaction coefficients of the equation; X_1, X_2 and X_3 are the levels of independent variables.

The EE of DOX in CMs-M-ALG-Beads was determined as previously reported.[20] Fifty milligrams of CMs-M-ALG-Beads were dissolved in 1 mL of hexafluoroisopropanol. The samples were shaken vigorously until complete dissolution of the polymers, added to 5 mL of dilute acetic acid, and incubated at 37 °C for 1 h, then, centrifuged at 12000 rpm for 30 min. To measure DOX concentration, the free DOX in supernatants was filtered through a membrane filter (0.45 μm), whose concentration was examined spectrophotometrically at 481 nm (UV-1100, Shimadzu, Kyoto, Japan). The *EE* was calculated using eq 2:

$$\text{EE}\ (\%) = (\text{Dose}_{\text{added}} - \text{Does}_{\text{free}})/\text{Dose}_{\text{added}} \times 100\% \quad (2)$$

where $\text{Dose}_{\text{added}}$ is total amount of DOX added, which contains the dose in core and in layer, and $\text{Dose}_{\text{free}}$ is free DOX in solution.

Swelling Studies. The swelling capability of CMs-M-ALG-Beads was evaluated in various pH media with different enzymes, simulating the complete gastrointestinal (GI) tract environment.[21,22] The following simulated fluids used were: simulated gastric fluid at pH 1.2 for 2 h, simulated duodenum fluid at pH 6.0 for 2 h, simulated jejunum fluid at pH 7.0 for 2h, and simulated ileum fluid at pH 7.4 for 2 h. The ingredients of simulated fluids were as follows:

- Simulated gastric fluid (SGF, pH 1.2): NaCl (0.2 g), HCl (7 mL), and pesin (3.2 g); pH was adjusted by NaOH to 1.2 ± 0.5.
- Simulated intestinal fluid (SIF, pH 7.4): KH_2PO_4 (6.8 g), 0.2 N NaOH (190 mL), and pancreatin (10.0 g).
- Simulated duodenum fluid (pH 6.0) was prepared by mixing SGF pH 1.2 and SIF pH 7.4 in a ratio of 30:70.
- Simulated jejunum fluid (pH 7.0): SIF adjusted by NaOH to 7.0 ± 0.1
- Simulated ileum fluid: SIF adjusted by NaOH to 7.4 ± 0.1.

Briefly, freeze-dried CMs-M-ALG-Beads were immersed in corresponding swelling medium and shaken (100 rpm) at 37 °C. At specific time intervals (every 30 min), the beads were removed, blotted with filter paper to remove moisture adhering to the surface immediately, and then weighed.[23] All experiments were done in triplicate. The swelling index (S_w) was determined according to eq 3:

$$S_w = (W_s - W_0)/W_0 \times\times 100\% \quad (3)$$

where W_s is the weight of the swelling bead, and W_0 is the weight of the freeze-dried bead.

To further study the pH responsiveness of CMs-M-ALG-Beads, the swelling characteristics of four-layer CMs-M-ALG-Beads were also examined at 37 °C in different swelling media (tris-HCl at pH 1.2, PBS at pH 6.0, PBS at pH 7.0 and 7.4) for 8 h, respectively. At a predetermined time (0 h, 2 h, 4 h, 6 and 8 h) in different swelling media, the morphology of the CMs-M-ALG-Beads was observed and imaged.

DOX Release in Simulated GI Fluid. To investigate the drug release process and track the DOX:CS/CMCS-CMs in CMs-M-ALG-Beads, CMCS was covalently labeled with fluorescein isothiocyanate (FITC) through amide bond formation between primary amino group on CMCS and isothiocyanate group on FITC at pH 6.9, and then dialyzed in tridistilled water for 3 days to remove unreacted FITC refer to previous report.[10] FITC-CMCS was able to form fluorescent DOX:CS/FITC-CMCS-CMs with DOX, and then immobilized in the multilayer ALG beads to form FITC-CMs-M-ALG-Beads as above-mentioned. At a predetermined time (0 h, 2 h, 4 h, 6 and 8 h) in simulated GI fluid, the release buffer was observed by transmission electron microscope (TEM, JEM-1200EX, JEOL Ltd., Japan) and CLSM, respectively.

In vitro release of DOX from CMs-M-ALG-Beads was evaluated in simulated GI fluid. The beads were placed into a cellulose membrane dialysis tube (molecular weight cutoff 8000−10 000).[24] The dialysis tube was placed in 50 mL of different simulated fluid and gently shaken in a thermostatted shaker bath at 37 °C, 50 rpm. Samples were removed at appropriate intervals and the amount of DOX released in the medium was determined spectrophotometrically at 481 nm. Calibration curves of DOX in Simulated GI Fluid were shown in Figure S1 in the Supporting Information. All procedures were carried out in the dark, and carbon dioxide blowing to avoid photodegradation of DOX.

Mucin Adsorption. The mucin adsorption of CMs-M-ALG-Beads was investigated according to the reported method[25,26] with some modification. CMs-M-ALG-Beads (10 mg) were dispersed in 3 mL mucin aqueous solution at different concentration (0.025, 0.05, 0.1, 0.2, and 0.5 mg/mL) (test group). The mucin aqueous solution without CMs-M-ALG-Beads at corresponding concentration of mucin was used as control. All samples were shaken at 37 °C for 30 min. Then the mucin in solution was measured by with a colorimetric method using periodic acid/Schiff staining. The absorbed mucin was calculated by the amount of free mucin in the test group from the amount of mucin in the control group.

Intestinal Adhesion. Fasted Sprague−Dawley rats (SD rats, 180 − 220 g) were anesthetized by an intraperitoneal injection of 40 mg/kg sodium pentobarbital, and a midline incision was made in the abdomen. DOX:CS/FITC-CMCS-CMs and FITC-CMs-M-ALG-Beads at the same dose of DOX:CS/FITC-CMCS-CMs (1 mg/mL, 1 mL) were syringed into a 6-cm duodenal, jejunal, or ileal sac and incubated in oxygenated Kreb's-Ringer buffer at 37 °C with smooth shaking. After 2 h incubation, the duodenal, jejunal, or ileal sac was washed with saline, and the detached DOX:CS/FITC-CMCS-CMs were collected for quantification of FITC-CMCS using spectrofluorimetry. Mucoadhesion of the DOX was calculated as eq 4

$$\text{Mucoadhesive capacity}\ (\%) = (W_{\text{initial}} - W_{\text{washed}})/W_{\text{initial}} \times 100\% \quad (4)$$

DOX Permeation. DOX:CS/CMCS-NGs, NGs-M-ALG-Beads, or DOX at the same dose of DOX (1 mg/mL) were syringed into a 6-cm duodenal, jejunal, or ileal sac and incubated in oxygenated Kreb's-Ringer buffer at 37 °C with smooth shaking. During 2 h of incubation, the DOX concentration in the incubation buffer was measured by a flourescence microplate reader at Ex/Em 537/584 nm (FLx800, BioTek, USA). The apparent permeability coefficient (P_{app}, cm/s) was calculated by eq 5:

$$P_{app} = Q/Act \quad (5)$$

where Q is the total amount of DOX permeated (ng), A is the surface area of monolayer (cm^2), c is the initial concentration of DOX over the apical side (μg/mL), and t is the time of the experiment (s).

Statistical Analysis. The assays were performed at least in triplicate on separate occasions. Statistical analysis of the differences in the measured properties of the groups was performed with one way analysis of variance and the determination of confidence intervals with the statistical package SigmaPlot, version 11.0 (Systat Software Inc., US). The data collected in this study was expressed as means and standard deviations, indicated as "mean ± SD". Differences were considered to be statistically significant when the P values were less than 0.05.

RESULTS AND DISCUSSION

Preparation and Characterization of CMs-M-ALG-Beads. CMs-M-ALG-Beads were prepared by immobilization of DOX:CS/CMCS-CMs in the core and layers of multilayer ALG beads. First, DOX:CS/CMCS-CMs were prepared by simple ionic gelation method as our recent report.[9] Then the DOX:CS/CMCS-CMs were immobilized in the ALG bead by dropping ALG and DOX:CS/CMCS-CMs mixture solution into $CaCl_2$ solution to form core bead (Scheme 1). During the coating process, part of the ALG and DOX:CS/CMCS-CMs mixture solution would be attracted on the surface of core bead after the core beads were immersed in the ALG + DOX:CS/CMCS-CMs mixture solution. Then, the beads were separated from each other and suspended in oil phase after they were

dx.doi.org/10.1021/bm401890x | *Biomacromolecules* XXXX, XXX, XXX−XXX

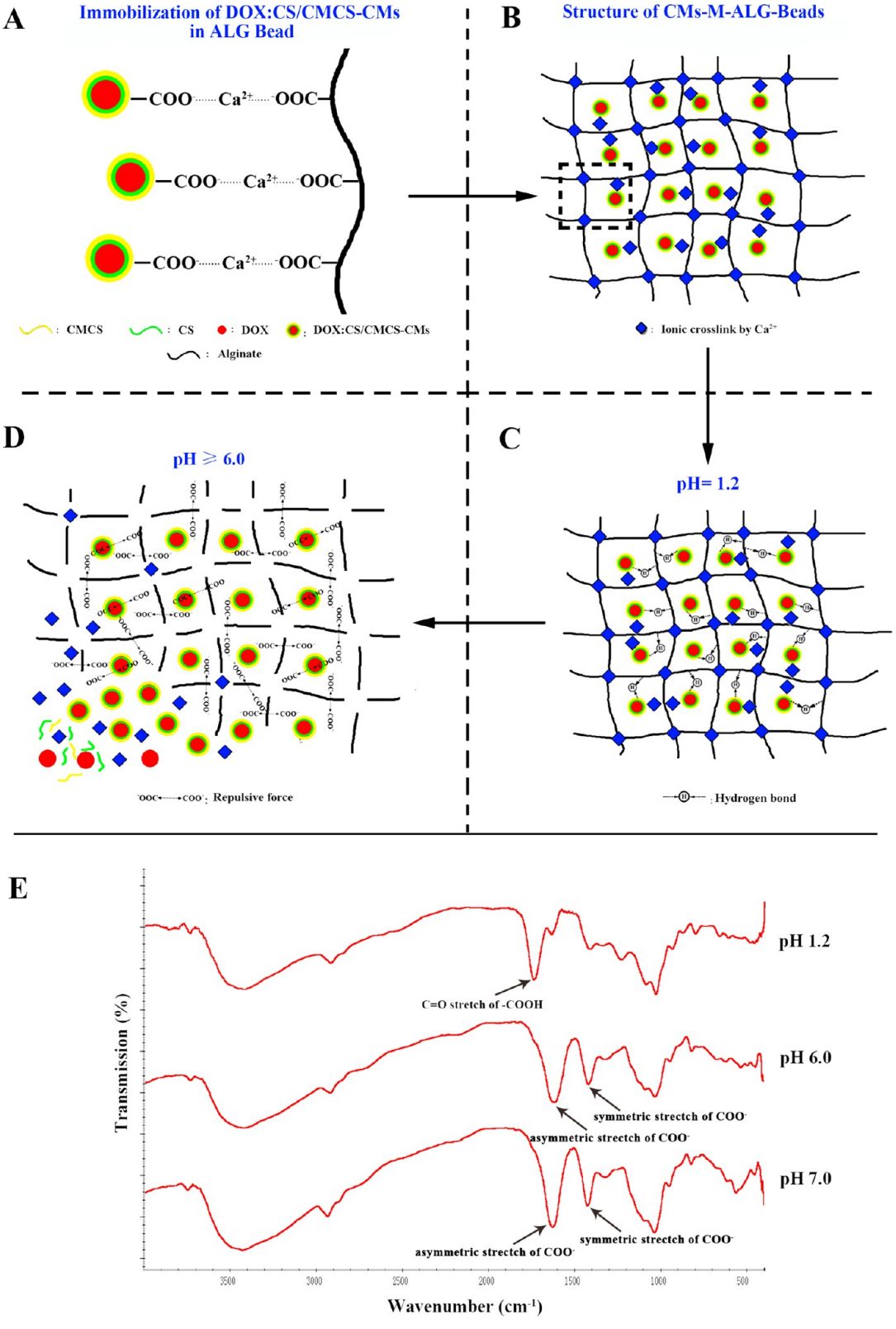

Figure 1. Schematic illustrations of the physical structures of DOX:CS/CMCS-CM-immobilized multilayer ALG bead (CMs-M-ALG-Bead): (A) Ionically cross-linking between DOX:CS/CMCS-CMs and ALG matrix. Structures of CMs-M-ALG-Bead at prepared condition (B), pH 1.2 (C) and pH ≥ 6.0 (D). (E) FT-IR spectra of CMs-M-ALG-Beads at pH 1.2, pH 6.0, and pH 7.4.

poured into oil phase. As the $CaCl_2$ was added to the mixture, the alginate solution would again cross-link with Ca^{2+}, and a layer was formed. Repeating the coating process, CMs-M-ALG-Beads with the required number of layers could be prepared.

The contact between alginate and Ca^{2+} in solution immediately induces ionic cross-links of alginate, thus forming encapsulated beads.[27,28] Gel formation was observed upon addition of aqueous CMCS into a calcium chloride solution,[29]

dx.doi.org/10.1021/bm401890x | *Biomacromolecules* XXXX, XXX, XXX−XXX

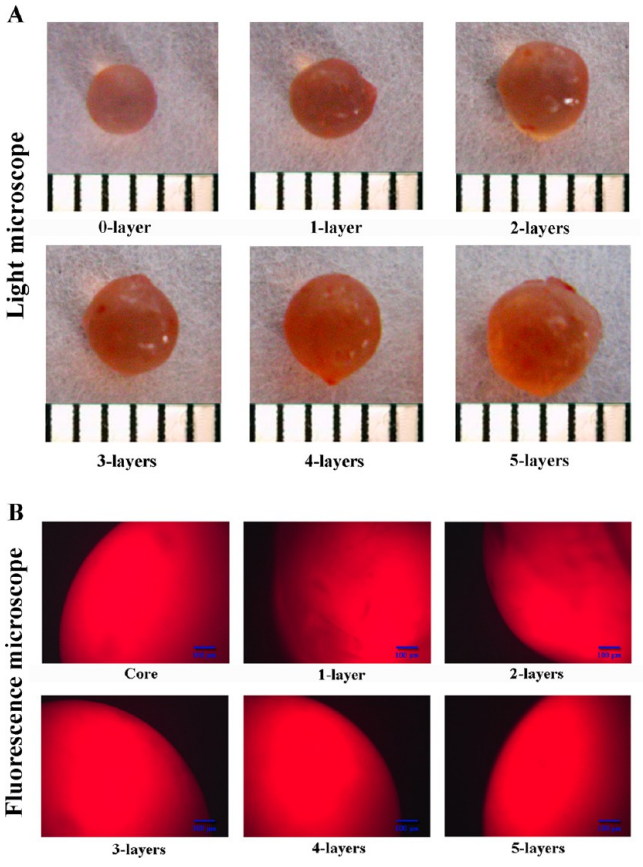

Figure 2. (A) Photographs of a swollen DOX:CS/CMCS-CM-immobilized multilayer ALG bead (CMs-M-ALG-Bead) with different numbers of layers. (B) Fluorescent image of a swollen CMs-M-ALG-Bead with different numbers of layers.

which indicated that ionic cross-links between the carboxylate ions ($-COO^-$) on CMCS can also be established by Ca^{2+}. Our previous study showed that CS/CMCS-CMs were negative charged because of the present of CMCS molecules on the surface of CMs.[9] Thus, in the preparation of the CMs-M-ALG-Beads, the $-COO^-$ on CMCS in DOX:CS/CMCS-CMs and $-COO^-$ on ALG matrix could be cross-linked by Ca^{2+} (Figure 1A), resulting in the formation of DOX:CS/CMCS-CM-immobilized multilayer ALG beads (Figure 1B).

The peak variation in the CMs-M-ALG-Beads at specific pH was examined by FT-IR (Figure 1E). At pH 1.2, the characteristic peaks observed at 1738 cm^{-1} were the carboxylic acids ($-COOH$) on alginate and CMCS. At pH 6.0 and pH 7.0, the carboxylic acid groups ($-COOH$) on alginate and CMCS became progressively ionized, and thus the asymmetric (1600 cm^{-1}) and symmetric (1418 cm^{-1}) stretching of carboxylate anion ($-COO^-$) on CMCS in DOX:CS/CMCS-CMs and the ALG matrix were observed, respectively. Therefore, at pH 1.2, there were hydrogen-bond formations between $-COOH$ and $-OH$ groups as well as ionic cross-links by Ca^{2+} between the carboxylate ions ($-COO^-$) on ALG and CMCS in DOX:CS/CMCS-CMs (Figure 1C). In contrast, at pH 6.0 and 7.0, a large expulsive force created by the electrostatic repulsion between the ionized acid groups ($-COO^-$) (Figure 1D).

CMs-M-ALG-Beads with different number of layers were spherical and nonaggregated (Figure 2A). Fluorescent images indicated that DOX:CS/CMCS-CMs were successfully immobilized in multilayer ALG bead, with no sign of partial or

Table 1. Mean Particle Sizes (n > 100) and DOX Encapsulation Efficiency (EE) (n = 5) of DOX:CS/CMCS-CM-Immobilized Multilayer ALG Beads

number of layers	mean particle size (mm)	EE (%)
0	2.78 ± 0.14	97.21 ± 1.3
1	3.13 ± 0.11	96.21 ± 2.2
2	3.47 ± 0.21	96.17 ± 2.9
3	3.83 ± 0.13	95.94 ± 1.8
4	4.21 ± 0.18	95.47 ± 2.1
5	4.59 ± 0.22	94.93 ± 3.2

Table 2. Variables in Box−Behnken Design

	levels used, actual (coded)		
independent variables	low	medium	high
X_1 = sodium alginate (% w/v)	1	3	5
X_2 = calcium chloride (% w/v)	1	3	5
X_3 = DOX:CS/CMCS-CMs (% w/v)	0.1	0.3	0.5
dependent variables	constraints		
Y = encapsulation efficiency (%)	maximize		

Table 3. Observed Responses in Box−Behnken Design

	independent variables			dependent variables
batch	X_1	X_2	X_3	Y
1	3	1	0.5	55.67
2	1	5	0.3	63.28
3	1	1	0.3	40.89
4	3	5	0.5	67.21
5	5	3	0.5	76.89
6	5	3	0.1	70.49
7	5	1	0.3	67.54
8	1	3	0.1	63.78
9	3	5	0.1	70.49
10	3	1	0.1	56.87
11	5	5	0.3	68.25
12	1	3	0.5	53.37
13[a]	3	3	0.3	95.69
14[a]	3	3	0.3	96.03
15[a]	3	3	0.3	97.73
16[a]	3	3	0.3	95.98
17[a]	3	3	0.3	95.34

[a]Indicates the center point of the design.

incomplete encapsulation of DOX (Figure 2B). The LBL structure could be seen clearly and separated after lyophilization of CMs-M-ALG-Beads (Figure 3A). The CLSM image of dry CMs-M-ALG-Beads suggested that DOX:CS/CMCS-CMs was located in the core and layer of multilayer ALG beads (Figure 3B, red fluorescent). The blank multilayer ALG bead (without DOX:CS/CMCS-CMs) exhibited smooth morphology with relatively few small depressions on the surface (Figure 3C). By contrast, the DOX:CS/CMCS-CM-immobilized multilayer ALG bead presented a rough surface structure with many small particles due to the presence of DOX:CS/CMCS-CMs in the layer. The above results indicated that DOX:CS/CMCS-CMs were successfully immobilized in the multilayer ALG bead.

The particle size of the CMs-M-ALG-Bead increased from 2.78 ± 0.14 mm to 4.59 ± 0.22 mm with increasing the number of layers (from 0 to 5 layers, Table 1). The particle size had a correlation with the initial drop size, the concentration of $CaCl_2$ and ALG, and the time of solidification, besides the number of

dx.doi.org/10.1021/bm401890x | Biomacromolecules XXXX, XXX, XXX−XXX

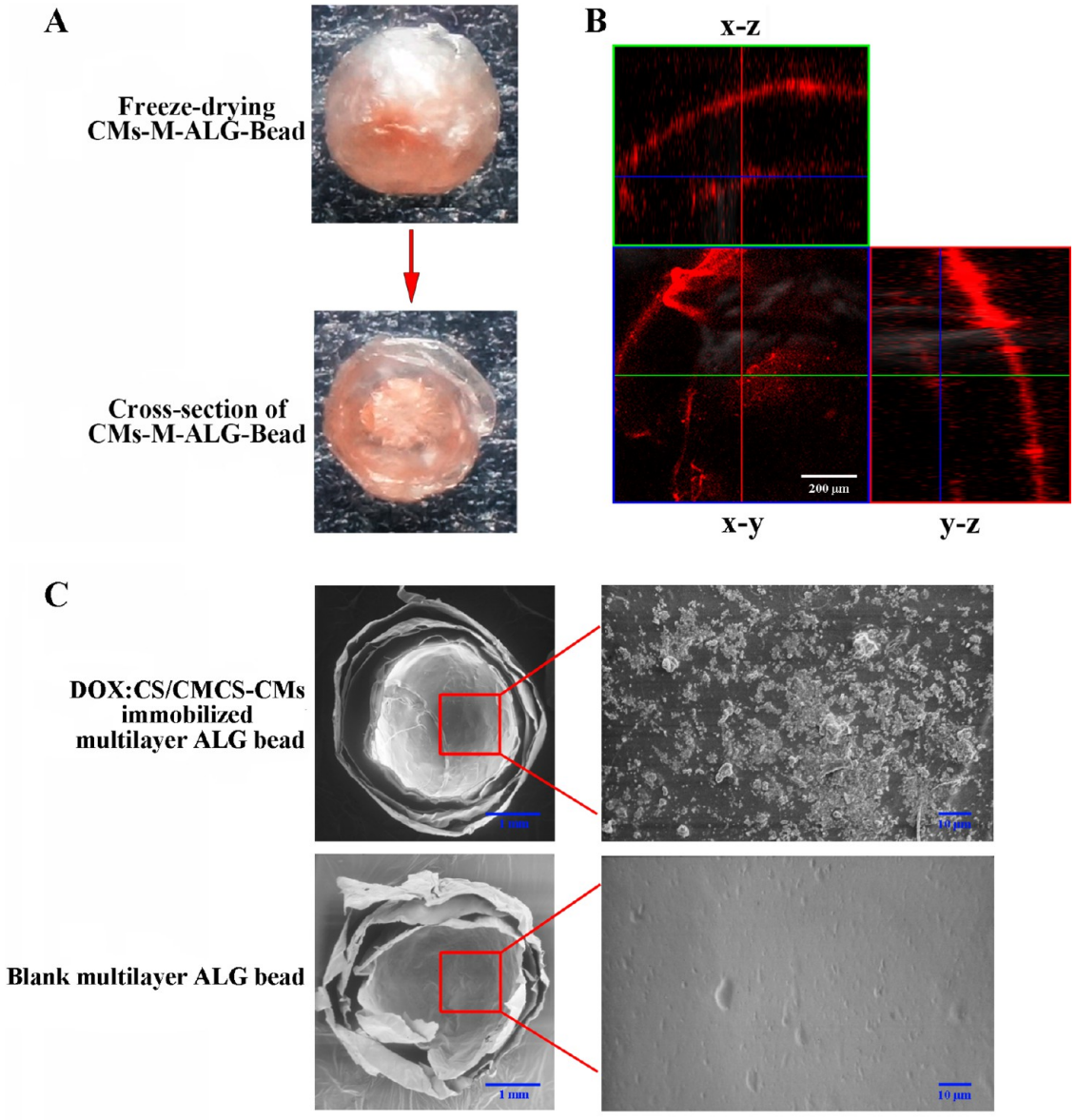

Figure 3. (A) Photograph of a freeze-dried four-layer CMs-M-ALG-Bead. (B) CLSM image of the cross-section of a freeze-dried four-layer DOX:CS/CMCS-CM-immobilized multilayer ALG bead (CMs-M-ALG-Bead). (C) SEM of the cross-section of a four-layer multilayer ALG bead with or without DOX:CS/CMCS-CMs.

layer. The appropriate concentration of alginate must be controlled in the range of 1−3%. Low alginate concentration (<1%) brings on the dilute gelling, resulting in no layer out of core bead. On the contrary, high alginate concentration (>3%) leads to high viscosity, which prevents the formation of core beads.

Optimization of Drug Encapsulation Efficiency of CMs-M-ALG-Beads. To achieve the maximum encapsulation efficiency of DOX, the response surface methodology (RSM) followed by Box−Behnken design was applied to find the optimal level of independent variables including ALG (%), $CaCl_2$ (%) and DOX:CS/CMCS-CMs (%) shown in Table 2. The range of the encapsulation efficiency was 53.37−97.73% (Table 3). A full quadratic second-order polynomial equation was fitted to the data appropriately (Table 4). The lack of fit *F*-value was 0.18 (Table 4), which implied that it was not significant in responses, due to the pure error and showed adequacy of the models.[30] Meanwhile, the multiple regression analysis showed that all the linear, squared, and interaction coefficients of the independent factors including ALG (%), $CaCl_2$ (%) and DOX:CS/CMCS-CMs (%) were significant ($p < 0.05$). Thus, the equation fitted to the data as eq 6:

$$Y = -38.20606 + 28.89988 \times X_1 + 37.08925 \times X_2 + 172.44250 \times X_3 - 1.35500 \times X_1 \times X_2 + 10.56250 \times X_1 \times X_3 - 4.02394 \times X_1^2 - 5.01706 \times X_2^2 - 347.58125 \times X_3^2 \quad (6)$$

where Y is EE, X_1, X_2, and X_3 are concentration of sodium alginate (%), calcium chloride (%), and DOX:CS/CMCS-CMs (%), respectively.

The coefficient of determination (R^2) and adjusted R^2 of this model were 0.9992 and 0.9984, respectively (Table 4). These suggested that almost 100% variability in the response will be explained by this model. The predicted R^2 with the value of

dx.doi.org/10.1021/bm401890x | *Biomacromolecules* XXXX, XXX, XXX−XXX

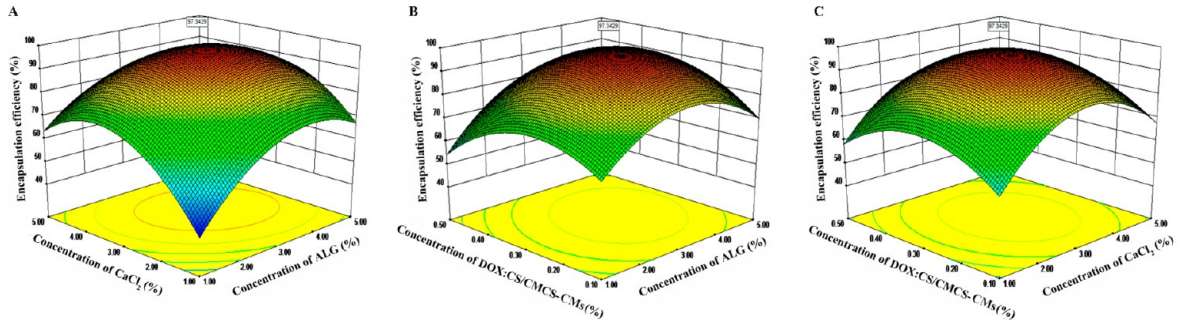

Figure 4. The response surface plot and the corresponding contour plot showing the effects of concentration of ALG (%), concentration of $CaCl_2$ (%), and concentration of DOX:CS/CMCS-CMs (%) on the encapsulation efficiency of DOX (%).

Table 4. The Analysis of Variance Table for Encapsulation Efficiency as the Response (Y)

source	sum of squares	df	mean square	F value	p value[a] prob > F
model	4955.47	9	550.61	993.74	<0.0001
A-SC	476.79	1	476.79	860.51	<0.0001
B-CA	273.20	1	273.20	493.06	<0.0001
C-DOX	6.25	1	6.25	11.28	0.0121
AB	117.51	1	117.51	212.07	<0.0001
AC	71.40	1	71.40	128.87	<0.0001
A^2	1090.83	1	1090.83	1968.74	<0.0001
B^2	1695.72	1	1695.72	3060.45	<0.0001
C^2	813.90	1	813.90	1468.92	<0.0001
residual	3.88	7	0.55		
lack of Fit	0.47	3	0.16	0.18	0.9018
pure Error	3.41	4	0.85		
cor total	4959.35	16			
R^2	0.9992				
adj. R^2	0.9984				
predicted R^2	0.9976				

[a]Significant at the 0.05 level.

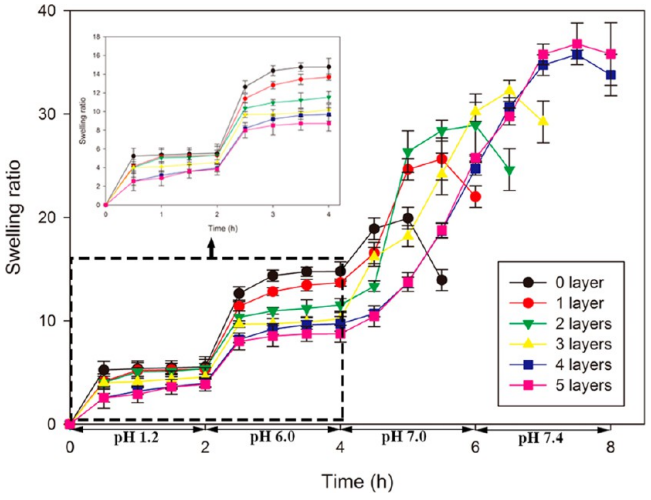

Figure 5. Swelling characteristics of DOX:CS/CMCS-CM-immobilized multilayer ALG beads with zero to five layers in the simulated fluid of the GI tract. (n = 4).

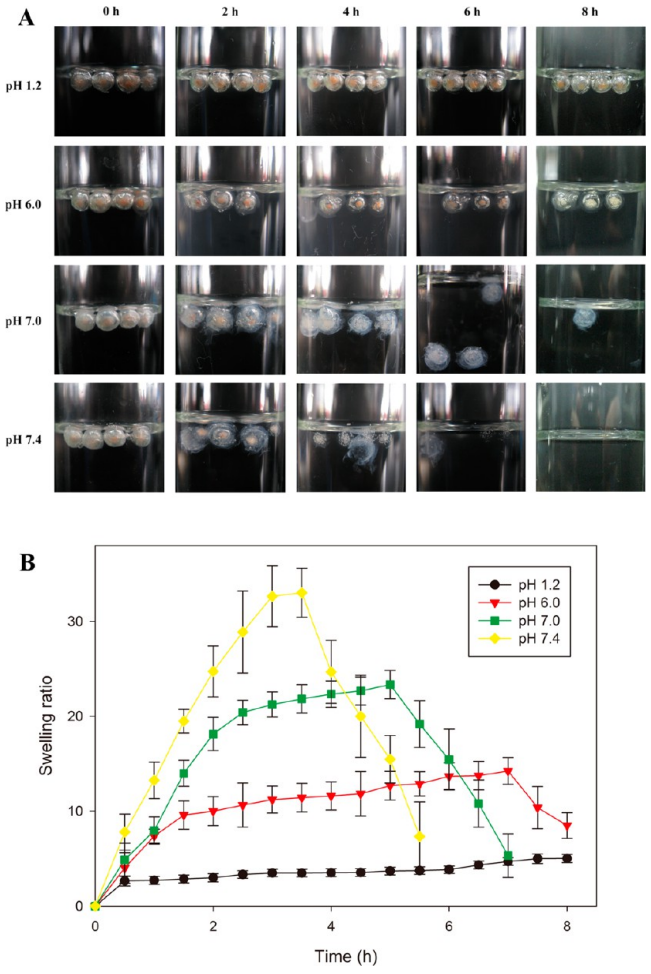

Figure 6. (A) Photographs of four-layer DOX:CS/CMCS-CM-immobilized multilayer ALG bead (CMs-M-ALG-Beads) in tris-HCl at pH 1.2, PBS at pH 6.0, pH 7.0 and pH 7.4, respectively. (B) Swelling characteristics of four-layer CMs-M-ALG-Beads in tris-HCl at pH 1.2, PBS at pH 6.0, and PBS at pH 7.0, respectively. (n = 5).

0.9976 showed very good agreement between the predicted and the experimental data.

The 3-D response surfaces of the independent variables on response Y were shown in Figure 4A–C. In each plot, the effect of two variables on Y was investigated, while the third one was kept at a middle level. All the relationships among the three variables were nonlinear, and it was observed that at lower $CaCl_2$ concentration, the EE of DOX increased with increasing concentrations of either ALG or DOX:CS/CMCS-CMs up to intermediate concentrations and then decreased at the combination of the high level of variables. Very high concentration of $CaCl_2$ led to low DOX EE because the excessive cross-linking between Ca^{2+} and ALG decreased the capacity of ALG beads to

dx.doi.org/10.1021/bm401890x | Biomacromolecules XXXX, XXX, XXX–XXX

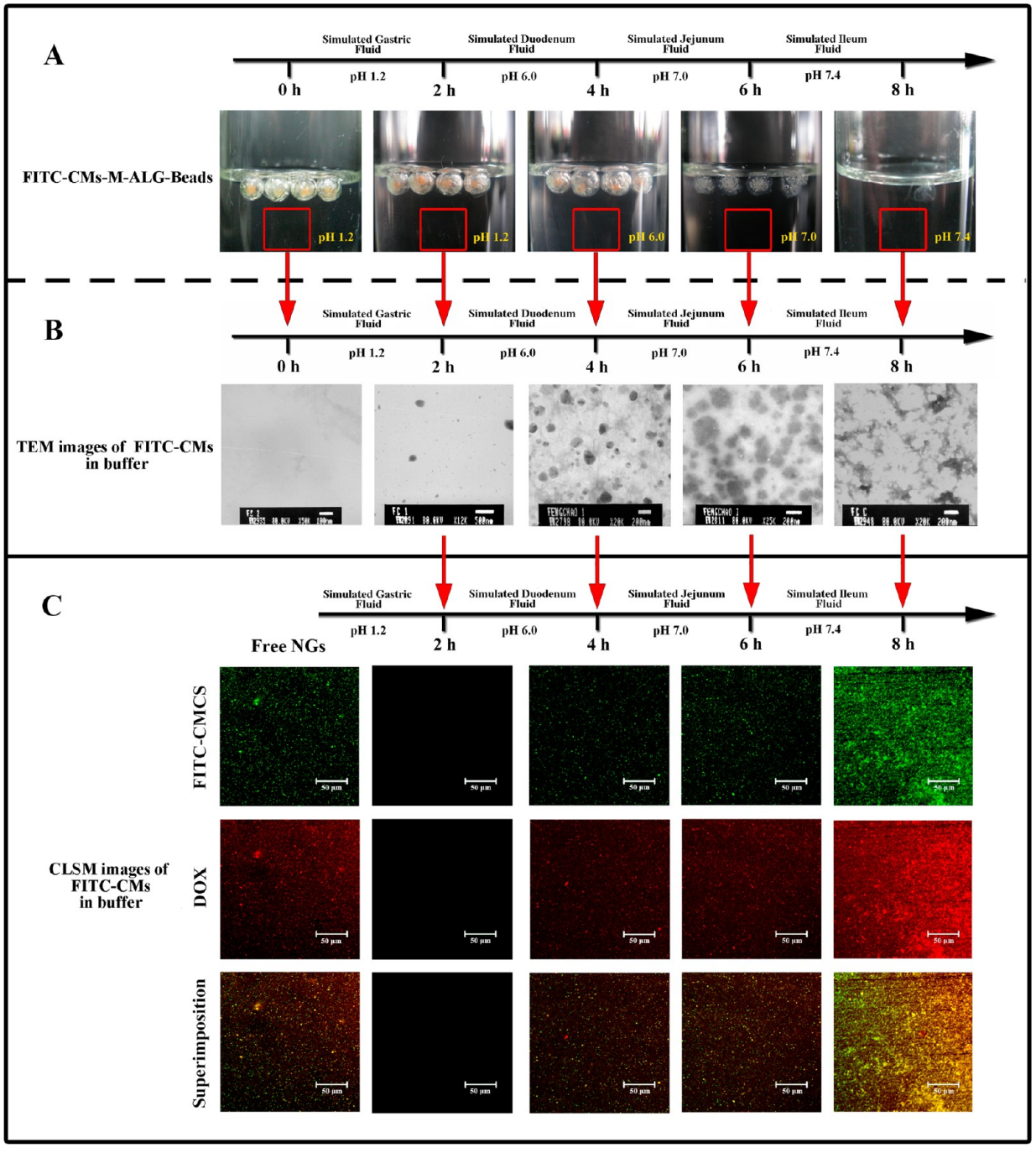

Figure 7. (A) Photographs of four-layer CMs-M-ALG-Beads in the simulated fluid of the GI tract and corresponding TEM (B) and CLSM (C) images of the release buffer.

immobilization of DOX:CS/CMCS-CMs, thus, decreased the encapsulation of DOX (Figure 4A, B). Meanwhile, higher concentrations of DOX:CS/CMCS-CMs resulted in lower encapsulation (Figure 4B and C) and a major proportion was washed away by water during the coating process.

By analysis of response surface plots obtained by Design-Expert software and the numerical solution for eq 6 and constraints, the optimum real values (actual) for independent variables to maximize the EE responses were obtained at ALG 3.44 (%), $CaCl_2$ 3.23 (%) and DOX:CS/CMCS-CMs 0.3 (%), respectively. The maximum predicted value of *EE* of CMs-M-ALG-Beads was estimated as 97.34%. To confirm the predicted results of the model, the repeated experiments under optimal conditions were carried out and an average value of 97.21% ± 1.3 (Table 1, 0-layer) was obtained. This result was obviously in close agreement with the model prediction. The perfect agreement between predicted and measured values verified the model validation.

The effect of the number of layers on the EE was shown in Table 1. No difference ($p > 0.05$) in EE of DOX between CMs-M-ALG-Beads with different layer numbers was observed. These results indicated that the DOX EE of CMs-M-ALG-Beads was not related to the number of layers. DOX:CS/CMCS-CMs were immobilized in core bead, and every layer of the multilayer ALG bead by electrostatic interaction between Ca^{2+} with carboxyl groups on ALG matrix and CMCS in DOX:CS/CMCS-CMs,

dx.doi.org/10.1021/bm401890x | *Biomacromolecules* XXXX, XXX, XXX−XXX

which only depends on the ratio of DOX:CS/CMCS-CMs, ALG, and Ca^{2+}.

Swelling Study. The swelling characteristics of CMs-M-ALG-Beads with zero to five layers were respectively studied simulating the GI tract (Figure 5). In stimulated gastric fluid (pH 1.2), three-, four-, and five-layer beads exhibited lower and approximately the same swelling ratio (no more than 5%) than other test beads. The minimal swelling ratio was beneficial for slowing down the rate of drug release. Therefore, the beads (three-, four- and five-layer) with low swelling rate at gastric acid could avoid the premature drug release in the gastric acid environment and enhance the efficiency of drug delivery. In simulated duodenum fluid (pH 6.0), jejunum fluid (pH 7.0), and simulated ileum fluid (pH 7.4), the swelling ratios of test beads increased significantly compared to those at pH 1.2 ($p < 0.05$). Additionally, disintegration of test multilayer beads was observed at the end of swelling. Unlike three-layer CMs-M-ALG-Beads, which started to disintegrate at pH 7.0, four- and five-layer CMs-M-ALG-Beads exhibited continuing swelling property within 1.5 h at pH 7.4. This character was beneficial to prolong the contact time between the DOX:CS/CMCS-CMs and the small intestine and thus enhance the absorption of drug. Meanwhile, no significant difference in swelling ratio was observed between four-layer and five-layer beads. Therefore, four-layer CMs-M-ALG-Beads were selected for further study.

To further investigate the pH responsiveness of CMs-M-ALG-Beads, the swelling characteristics of four-layer CMs-M-ALG-Beads were studied at different pH environment for 8 h, respectively (Figure 6B), and the corresponding images were taken at 0 h, 2 h, 4 h, 6 h, and 8 h (Figure 6A). At pH 1.2, the four-layer CMs-M-ALG-Beads were spherical and compact for 8 h, and their swelling ratio was lower than 5% due to the intramolecular- and intermolecular-hydrogen bond between −COOH and −OH groups and the ionic cross-links by Ca^{2+} between the carboxylate ions ($-COO^-$) on the ALG matrix and CMCS in DOX:CS/CMCS-CMs. At pH 6.0, hydrogen bonds were broken as a result of the deprotonation of −COOH groups. The swelling ratio was significantly higher than that in pH 1.2, and the size of CMs-M-ALG-Beads increased with the increase of the swelling time. This phenomenon was attributed to the repulsive force produced by the deprotonation carboxyl group ($-COO^-$) on the ALG matrix and CMCS in DOX:CS/CMCS-CMs. However, no disintegration was observed at pH 6.0 during 8 h, which might be caused by ionic cross-links by Ca^{2+} within the test beads and strong electrostatic interaction between the protonated $-NH_3^+$ groups on CS and CMCS in DOX:CS/CMCS-CMs with deprotonated carboxyl groups ($-COO^-$) on ALG. At pH 7.0 and 7.4, $-NH_3^+$ groups on CS and CMCS in DOX:CS/CMCS-CMs had completely deprotonized, which weakened the electrostatic interaction. In addition, the Ca^{2+} was sequestrated from the ALG matrix by phosphates and replaced by sodium, leading to the dissolution of ALG. Therefore, swelling of the CMs-M-ALG-Beads was limited and started to disintegrate within 2 h (at pH 7.0) or 1.5 h (at pH 7.4).

DOX Release in Vitro. To track the DOX:CS/CMCS-CMs released from CMs-M-ALG-Beads, the DOX:CS/FITC-CMCS-CMs were prepared and immobilized in four-layer ALG beads to form FITC-CMs-M-ALG-Beads. The photographs of four-layer FITC-CMs-M-ALG-Beads in simulated GI fluid were taken (Figure 7A) at predetermined times (0 h, 2 h, 4 h, 6 h, and 8 h). The corresponding release buffer was also observed by TEM (Figure 7B) and CLSM (Figure 7C), respectively. For CLSM image, the overlap of red (DOX-related fluorescence) and green (FITC-CMCS in DOX:CS/FITC-CMCS-CMs) fluorescence

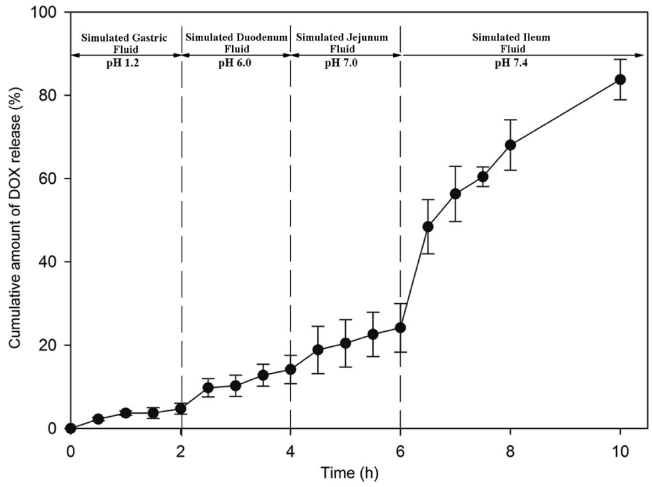

Figure 8. (A) Release profiles of DOX from four-layer DOX:CS/CMCS-CM-immobilized multilayer ALG beads in the simulated fluid of the GI tract. ($n = 5$).

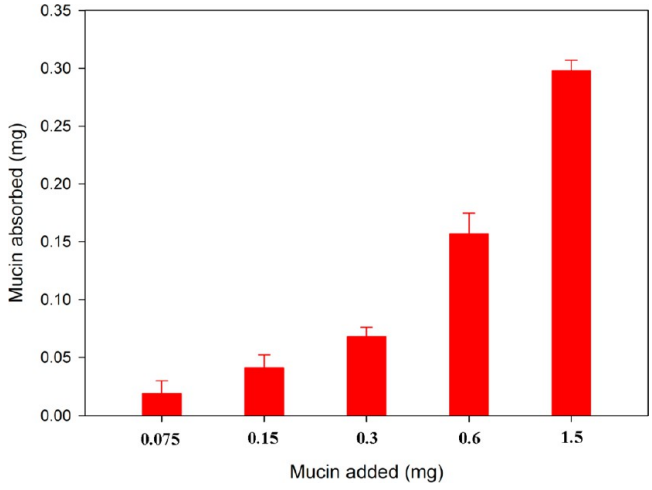

Figure 9. Adsorption of mucin on DOX:CS/CMCS-CM-immobilized ALG multilayer beads. ($n = 5$).

appeared as a yellow spot that indicated the integrity of the DOX:CS/FITC-CMCS-CMs. The beads maintained spherical shape (Figure 7A) after 2 h incubated in stimulated gastric fluid. TEM and CLSM results showed that no free DOX:CS/FITC-CMCS-CMs were observed in release buffer (Figure 7B,C). Then, after 2 h of incubation in stimulated duodenum fluid, the structure of beads still maintained integrity, but a number of intact DOX:CS/FITC-CMCS-CMs were observed in release buffer by TEM and exhibited a yellow spot in the CLSM image. After 2 h of incubation in stimulated jejunum fluid, the beads became disintegrated, and more intact DOX:CS/FITC-CMCS-CMs were found in release buffer. Finally, after 2 h of incubation in stimulated ileum fluid, the beads disappeared, and the DOX:CS/FITC-CMCS-CMs were completely released and exhibited strong fluorescence in the CLSM image. These results indicated that the DOX could be released from the CMs-M-ALG-Beads after two steps. First, DOX:CS/CMCS-CMs gradually escaped from the multilayer beads with the disintegration of multilayer ALG beads in the small intestine. Then, DOX was released from DOX:CS/CMCS-CMs when the CMs infiltrated into the mucus layer and approach enterocytes.

dx.doi.org/10.1021/bm401890x | *Biomacromolecules* XXXX, XXX, XXX−XXX

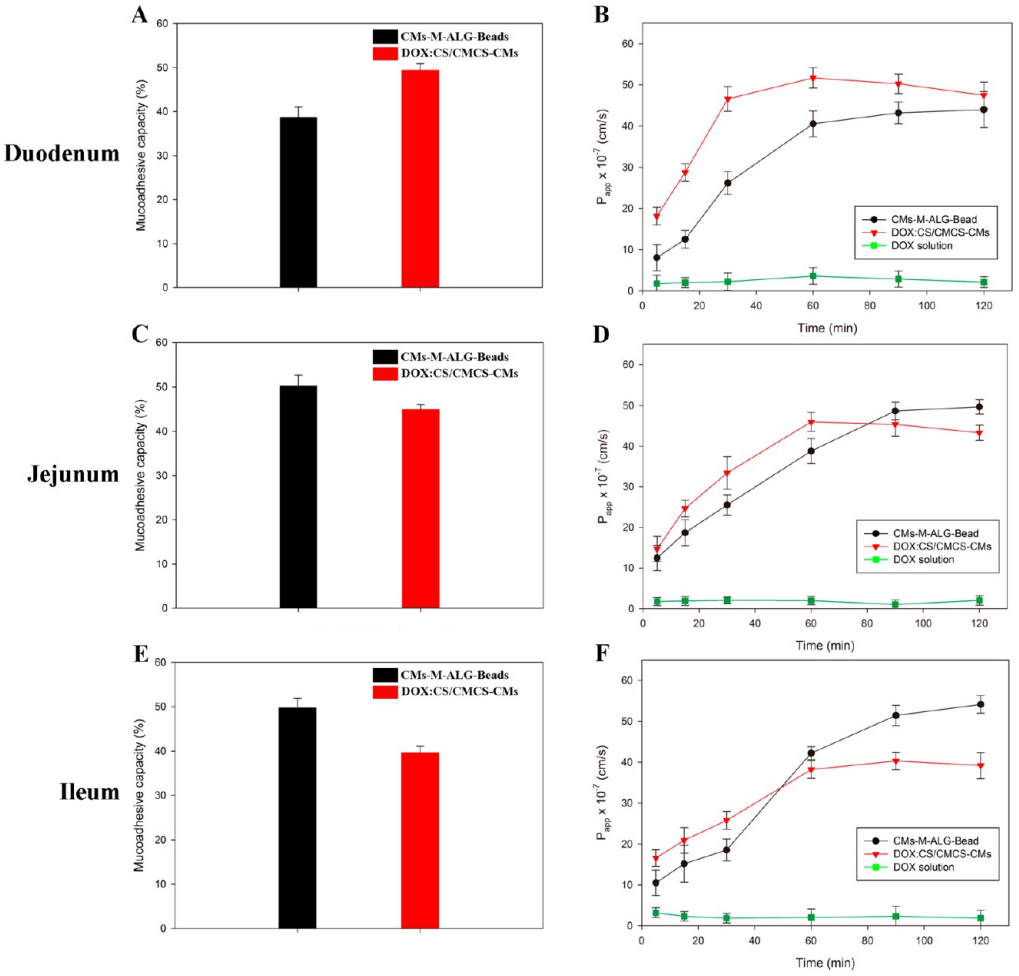

Figure 10. Ex vivo mucoadhesion of DOX, DOX:CS/CMCS-CMs, and CMs-M-ALG-Beads in different segments of small intestine of rate (A: duodenum, C: jejunum, E: ileum) (n = 4). Apparent permeability coefficients (P_{app}) for DOX in different segments of small intestine of rat from DOX, DOX:CS/CMCS-CMs, and CMs-M-ALG-Beads (B: duodenum, D: jejunum, F: ileum) (n = 4).

The corresponding successive DOX release characteristics of four-layer CMs-M-ALG-Beads were studied in vitro, simulating the GI tract (Figure 8). In stimulated gastric fluid, the cumulative amount of DOX released from the CMs-M-ALG-Beads was no more than 3.8% due to the excellent protective effect of multilayer ALG matrix on DOX:CS/CMCS-CMs. In simulated duodenum fluid, although some of DOX:CS/CMCS-CMs were released from the ALG matrix with the swelling of multilayer ALG beads (Figure 7B,C), the DOX release ratio was no more than 12.6% (Figure 8). This was attributed to the sustained drug release ability of DOX:CS/CMCS-CMs. In simulated jejunum and ileum fluids, the disintegration of multilayer ALG beads led to a large release of DOX:CS/CMCS-CMs (Figure 7B,C); the cumulative amount of DOX released was increased significantly (Figure 8).

Mucin Adsorption. The mucoadhesive behavior of CMs-M-ALG-Beads was determined by incubating the suspension of the CMs-M-ALG-Beads in different amounts of an aqueous mucin solution at 37 °C and the corresponding concentration of mucin solution without CMs-M-ALG-Beads was used as a control (Figure 9, Table S1 in the Supporting Information). The amount of mucin adsorbed by CMs-M-ALG-Beads increased ($p < 0.05$) with the increase in concentration of mucin. This was attributed to the formation of a strong hydrogen bond between the carboxylate anion of the ALG matrix and CMCS in DOX:CS/CMCS-CMs with mucin.[31,32] Meanwhile, it is expected that mucin could be spontaneously adsorbed by CMs-M-ALG-Beads, due to the electrostatic attraction between the positive charged amino groups on CS and CMCS in DOX:CS/CMCS-CMs with the negatively charged sialic acid group on mucin.[26]

Intestinal Adhesion. The mucoadhesive capacity of DOX:CS/CMCS-CMs varied in different segments of the small intestine of rats. In the duodenum (Figure 10A), the mucoadhesive capacity of DOX:CS/CMCS-CMs treated with free DOX:CS/CMCS-CMs was significantly higher than that treated with CMs-M-ALG-Beads. It was attributed to the LBL structure of a multilayer bead delaying the DOX:CS/CMCS-CMs release from the multilayer ALG Beads at pH 6.0. However, in the jejunum and ileum (Figure 10C, E), the DOX:CS/CMCS-CMs were rapidly released from CMs-M-ALG-Beads. Meanwhile, the ALG matrix around the DOX:CS/CMCS-CMs was beneficial for improving the intestinal adhesion of DOX:CS/CMCS-CMs.[33] Thus, CMs-M-ALG-Beads exhibited higher mucoadhesive capacity of DOX:CS/CMCS-CMs, which were about 1.12-fold and 1.25-fold higher than that of free DOX:CS/CMCS-CM groups in the jejunum and ileum, respectively.

DOX Permeation. The time-dependent P_{app} of DOX in different segments of the small intestine of rats was shown in Figure 10B, D, F. For DOX solution, the amount of DOX in the serosal fluid increased slightly with time in all intestinal segments.

dx.doi.org/10.1021/bm401890x | Biomacromolecules XXXX, XXX, XXX−XXX

In comparison, the higher transport of DOX was achieved by using free DOX:CS/CMCS-CMs and CMs-M-ALG-Beads. In the duodenum (Figure 10B), the permeation of DOX treated with DOX:CS/CMCS-CMs was significantly higher than that treated with CMs-M-ALG-Beads. However, the difference between the free DOX:CS/CMCS-CMs and the CMs-M-ALG-Beads decreased with the increase of incubation time. In the jejunum and ileum (Figure 10D, F), decreased permeation of DOX treated with DOX:CS/CMCS-CMs was observed at the end of incubation. In contrast, CMs-M-ALG-Beads exhibited continued growth for P_{app} values of DOX, which was 1.07−1.15-fold and 1.28−1.38-fold higher than free DOX:CS/CMCS-CMs in rat jejunum and ileum, respectively.

In our recent study, DOX:CS/CMCS-CMs could enhance the absorption of DOX throughout the entire small intestine due to the synergy effect of CS in CMs and CMCS in CMs.[10] In this study, the DOX:CS/CMCS-CMs were immobilized in the ALG multilayer bead and exhibited a higher intestinal permeation and mucoadhesive than free DOX:CS/CMCS-CMs in jejunum and ileum. This phenomenon might be attributed to three aspects. First, the sustained release of DOX:CS/CMCS-CMs from the CMs-M-ALG-Beads could prolong the contact time between the DOX:CS/CMCS-CMs and small intestinal mucosal. Second, the formation of a strong hydrogen bond between the carboxylate anion of ALG and CMCS in DOX:CS/CMCS-CMs with mucin could increase the contact between DOX:CS/CMCS-CMs with intestinal mucosal. Finally, similar to CMCS, the high binding capacity to Ca^{2+} of deprotonated carboxyl groups on ALG could further enhance the absorption of DOX.

CONCLUSIONS

DOX:CS/CMCS-CMs were successfully immobilized in an ALG multilayer bead. The obtained CMs-M-ALG-Beads possessed excellent low pH tolerance to enhance the stability of DOX:CS/CMCS-CMs in the stomach and rapidly release intact DOX:CS/CMCS-CMs in the small intestine. By prolonging the contact time between the DOX:CS/CMCS-CMs and small intestine mucosal, CMs-M-ALG-Beads were able to enhance the absorption of DOX. These results suggest that CMs-M-ALG-Beads may be an effective and promising carrier for improving the efficacy and safety of orally administered anticancer drugs by targeting release of the drug-loaded CS/CMCS-CMs and enhancing the absorption of the drug in the small intestine. Additionally, CMs-M-ALG-Beads with LBL structure have the potential to deliver multiple drugs by encapsulating different drugs in the core and layers, respectively, which may be used in combined therapy.

ASSOCIATED CONTENT

Supporting Information

Supporting Information. Calibration curves of DOX in simulated GI Fluid and mucin absorption of DOX:CS/CMCS-CM-immobilized multilayer ALG beads.This material is available free of charge via the Internet at http://pubs.acs.org.

AUTHOR INFORMATION

Corresponding Authors

*Tel: +86-0532-82032586. Fax: +86-0532-82032586. E-mail: xgchen@ouc.edu.cn (X.G.C).

*E-mail: hjpark@korea.ac.kr (H.J.P).

Notes

The authors declare no competing financial interest.

ACKNOWLEDGMENTS

This work was supported by National Natural Science Foundation of China (No.81271727, 31240007), International Science Technology Cooperation Program of China (No.2013DFG32880), Ph.D. Programs Foundation of Ministry of Education of China (NO. 20120132110012) and Scholarship Award for Excellent Doctoral Student granted by Ministry of Education.

REFERENCES

(1) Mei, L.; Zhang, Z.; Zhao, L.; Huang, L.; Yang, X. L.; Tang, J.; Feng, S. S. Pharmaceutical nanotechnology for oral delivery of anticancer drugs. *Adv. Drug. Deliv. Rev.* **2013**, *65* (6), 880−90.

(2) O'Neill, V. J.; Twelves, C. J. Oral cancer treatment: developments in chemotherapy and beyond. *Br. J. Cancer* **2002**, *87* (9), 933−937.

(3) Allen, T. M.; Cullis, P. R. Drug Delivery Systems: Entering the Mainstream. *Science* **2004**, *303* (5665), 1818−1822.

(4) Thanki, K.; Gangwal, R. P.; Sangamwar, A. T.; Jain, S. Oral delivery of anticancer drugs: Challenges and opportunities. *J. Controlled Release* **2013**, *170* (1), 15−40.

(5) Feng, S.-S.; Mei, L.; Anitha, P.; Gan, C. W.; Zhou, W. Poly(lactide)−vitamin E derivative/montmorillonite nanoparticle formulations for the oral delivery of Docetaxel. *Biomaterials* **2009**, *30* (19), 3297−3306.

(6) Benival, D. M.; Devarajan, P. V. Lipomer of doxorubicin hydrochloride for enhanced oral bioavailability. *Int. J. Pharm.* **2012**, *423* (2), 554−61.

(7) Mazzaferro, S.; Bouchemal, K.; Ponchel, G. Oral delivery of anticancer drugs III: formulation using drug delivery systems. *Drug Discov. Today* **2013**, *18* (1−2), 99−104.

(8) Mazzaferro, S.; Bouchemal, K.; Ponchel, G. Oral delivery of anticancer drugs I: general considerations. *Drug Discov. Today* **2013**, *18* (1−2), 25−34.

(9) Feng, C.; Wang, Z. G.; Jiang, C. Q.; Kong, M.; Zhou, X.; Li, Y.; Cheng, X. J.; Chen, X. G. Chitosan/o-carboxymethyl chitosan nanoparticles for efficient and safe oral anticancer drug delivery: in vitro and in vivo evaluation. *Int. J. Pharm.* **2013**, *457* (1), 158−167.

(10) Feng, C.; Sun, G. H.; Wang, Z. G.; Cheng, X. G.; Park, H. J.; Cha, D. S.; Kong, M.; Chen, X. G., Transport mechanism of doxorubicin loaded chitosan based nanogels across intestinal epithelium. *Eur. J. Pharm. Biopharm.* **2013**, http://dx.doi.org/10.1016/j.ejpb.2013.11.007, in press.

(11) El-Sherbiny, I. M. Enhanced pH-responsive carrier system based on alginate and chemically modified carboxymethyl chitosan for oral delivery of protein drugs: Preparation and in-vitro assessment. *Carbohydr. Polym.* **2010**, *80* (4), 1125−1136.

(12) Cook, M. T.; Tzortzis, G.; Khutoryanskiy, V. V.; Charalampopoulos, D. Layer-by-layer coating of alginate matrices with chitosan-alginate for the improved survival and targeted delivery of probiotic bacteria after oral administration. *J. Mater. Chem. B* **2013**, *1* (1), 52−60.

(13) Zakharova, L. Y.; Ibragimova, A. R.; Vasilieva, E. A.; Mirgorodskaya, A. B.; Yackevich, E. I.; Nizameev, I. R.; Kadirov, M. K.; Zuev, Y. F.; Konovalov, A. I. Polyelectrolyte Capsules with Tunable Shell Behavior Fabricated by the Simple Layer-by-Layer Technique for the Control of the Release and Reactivity of Small Guests. *J. Phys. Chem. C* **2012**, *116* (35), 18865−18872.

(14) del Mercato, L. L.; Rivera-Gil, P.; Abbasi, A. Z.; Ochs, M.; Ganas, C.; Zins, I.; Sonnichsen, C.; Parak, W. J. LbL multilayer capsules: recent progress and future outlook for their use in life sciences. *Nanoscale* **2010**, *2* (4), 458−467.

(15) Tong, W.; Song, X.; Gao, C. Layer-by-layer assembly of microcapsules and their biomedical applications. *Chem. Soc. Rev.* **2012**, *41* (18), 6103−6124.

(16) Yu, L.; Gao, Y.; Yue, X.; Liu, S.; Dai, Z. Novel hollow microcapsules based on iron-heparin complex multilayers. *Langmuir* **2008**, *24* (23), 13723−9.

(17) Chen, X.-G.; Park, H.-J. Chemical characteristics of O-carboxymethyl chitosans related to the preparation conditions. *Carbohydr. Polym.* **2003**, *53* (4), 355−359.
(18) Zhou, X.; Cheng, X. J.; Liu, W. F.; Li, J.; Ren, L. H.; Dang, Q. F.; Feng, C.; Chen, X. G. Optimization and characteristics of preparing chitosan microspheres using response surface methodology. *J. Appl. Polym. Sci.* **2013**, *127* (6), 4433−4439.
(19) Motwani, S. K.; Chopra, S.; Talegaonkar, S.; Kohli, K.; Ahmad, F. J.; Khar, R. K. Chitosan-sodium alginate nanoparticles as submicroscopic reservoirs for ocular delivery: Formulation, optimization and in vitro characterisation. *Eur. J. Pharm. Biopharm.* **2008**, *68* (3), 513−525.
(20) Xu, Q.; Xia, Y.; Wang, C.-H.; Pack, D. W. Monodisperse double-walled microspheres loaded with chitosan-p53 nanoparticles and doxorubicin for combined gene therapy and chemotherapy. *J. Controlled Release* **2012**, *163* (2), 130−135.
(21) Saboktakin, M. R.; Tabatabaie, R. M.; Maharramov, A.; Ramazanov, M. A. Synthesis and in vitro evaluation of carboxymethyl starch-chitosan nanoparticles as drug delivery system to the colon. *Int. J. Biol Macromol.* **2011**, *48* (3), 381−385.
(22) Huang, X.; Xiao, Y.; Lang, M. Micelles/sodium-alginate composite gel beads: A new matrix for oral drug delivery of indomethacin. *Carbohydr. Polym.* **2012**, *87* (1), 790−798.
(23) Li, Y.; Kong, M.; Feng, C.; Liu, W. F.; Liu, Y.; Cheng, X. J.; Chen, X. G. Preparation and property of layer-by-layer alginate hydrogel beads based on multi-phase emulsion technique. *J. Sol-Gel. Sci. and Techn.* **2012**, *62* (2), 217−226.
(24) Zhang, J.; Chen, X. G.; Sun, G. Z.; Huang, L.; Cheng, X. J. Effect of molecular weight on the oleoyl-chitosan nanoparticles as carriers for doxorubicin. *Colloids Surf. B Biointerfaces* **2010**, *77* (2), 125−30.
(25) Dhawan, S.; Singla, A.; Sinha, V. Evaluation of mucoadhesive properties of chitosan microspheres prepared by different methods. *AAPS. PharmSciTech.* **2004**, *5* (4), 122−128.
(26) He, P.; Davis, S. S.; Illum, L. In vitro evaluation of the mucoadhesive properties of chitosan microspheres. *Int. J. Pharm.* **1998**, *166* (1), 75−88.
(27) Zhu, H.; Srivastava, R.; McShane, M. J. Spontaneous Loading of Positively Charged Macromolecules into Alginate-Templated Polyelectrolyte Multilayer Microcapsules. *Biomacromolecules* **2005**, *6* (4), 2221−2228.
(28) Mørch, Ý. A.; Donati, I.; Strand, B. L. Effect of Ca^{2+}, Ba^{2+}, and Sr^{2+} on Alginate Microbeads. *Biomacromolecules* **2006**, *7* (5), 1471−1480.
(29) Feng, C.; Chen, X.; Zhang, J.; Sun, G.; Cheng, X.; Wang, Z.; Park, H.-J. The effect of carboxymethyl-chitosan nanoparticles on proliferation of keloid fibroblast. *Front. Chem. China* **2011**, *6* (1), 31−37.
(30) Gazori, T.; Khoshayand, M. R.; Azizi, E.; Yazdizade, P.; Nomani, A.; Haririan, I. Evaluation of Alginate/Chitosan nanoparticles as antisense delivery vector: Formulation, optimization and in vitro characterization. *Carbohyd. Polym.* **2009**, *77* (3), 599−606.
(31) Taylor Nordgård, C.; Draget, K. I. Oligosaccharides As Modulators of Rheology in Complex Mucous Systems. *Biomacromolecules* **2011**, *12* (8), 3084−3090.
(32) Taylor, C.; Draget, K. I.; Pearson, J. P.; Smidsrød, O. Mucous Systems Show a Novel Mechanical Response to Applied Deformation. *Biomacromolecules* **2005**, *6* (3), 1524−1530.
(33) Tønnesen, H. H.; Karlsen, J. Alginate in Drug Delivery Systems. *Drug. Dev. Ind. Pharm* **2002**, *28* (6), 621−630.